

Recursive Adaptive Color KLT for image sequences

Roumen K. Kountchev and Roumiana A. Kountcheva

Abstract - The method *Recursive color space transform for a sequence of correlated RGB images* is based on the algorithm Adaptive Color KLT (AC-KLT). The non-recursive AC-KLT for a sequence of color images is not efficient enough in this case, because each image should be processed individually. Depending on the kind of the images in the processed sequence (for example, color video, multi-view, medical sequences, etc.), the pixels of same position, but from two neighbor images, have significant similarity which in most cases is over 90 %. In such case, strong possibility exists for high reduction of the information redundancy of the color information. To this end, here is offered the method Recursive AC-KLT (RAC-KLT) whose basic idea is to execute the AC-KLT for the first image in the sequence, and for the next images to calculate the values of the difference parameters only, which are needed for the successful restoration of the color information. The efficiency of the new method grows up together with the mutual correlation between the consecutive images in the sequence. The evaluation of the computational complexity of the new algorithm confirms its advantage towards the basic AC-KLT. In the paper are also given some experimental results from the comparison between color transforms YCrCb, AC-KLT and RAC-KLT which show the higher efficiency of the new approach. Here are also commented the possible application areas for efficient representation of correlated image sequences.

Keywords—Adaptive Color Space Transform, Karhunen-Loeve Transform, Recursive Adaptive Color KLT, Sequence of Correlated Color Images.

I. INTRODUCTION

The processing and analysis of sequences of correlated color images are recently the object of significant number of scientific investigations [1-4] aimed at the reduction of the color information redundancy, noise filtration, segmentation and objects recognition based on their color, tracing of moving objects in video sequences, analysis of the color characteristics in selected areas in a group of images, etc. One of the most efficient transforms of the initial colors space (RGB) is the Karhunen-Loeve Transform (KLT) [5-10] also known as Hotelling Transform (HT), or Principal Component Analysis (PCA). Its most important advantage towards the well-known deterministic color transforms YCrCb (the most commonly used color space for compression), YUV, YIQ, RCT, YCoCg,

RDgDb, HSV or HSL, CMY, PhotoYCC, Lab, Luv, etc. [2,3,8,12,13], is the maximum decorrelation of the transformed color components $L_1L_2L_3$. The main disadvantage of the color KLT is that it has higher computational complexity than the deterministic transforms. To partially overcome the problem, approximately optimal color KLT with fixed coefficients is presented in [8]. Another approach for KLT complexity reduction is given in [14], where it is used for recursive coding of image blocks of small size. In this case, the full transform is executed for the first block only, and for the next blocks are calculated the values of the difference parameters in respect to the previous. This approach was further developed in [15] for local adaptive color transform of blocks and was aimed at the image compression. In each block of the image the coefficients of the color transform matrix are determined from the previously compressed four neighbor blocks by using the weighted sums of the RGB pixel values, which makes the transform block-specific. The efficiency of the block coding is related to the spatial inter-block correlation, which depends on the image contents and in many cases could be not too high.

For a large part of the existing image sequences the correlation between pixels of same spatial position in two neighbor images is much higher than the inter-block correlation inside the image. To enhance the efficiency of the RGB components processing, for each pixel from a given image in the group here is offered to execute recursive calculation of the KLT transform matrix of size 3×3 . This approach is the basics of the method called *Recursive Adaptive Color KLT* (RAC-KLT), presented here. It is based on the adaptive RGB space transform for a single image, called Adaptive Color KLT (AC-KLT) [16], which has lower computational complexity than the famous KLT algorithms based on iterative computational methods [5,6]. Together with the fast development of the contemporary computer technologies the color space transform based on the AC-KLT becomes suitable for more application areas, where the processing time satisfies the real-time implementation requirements.

The paper is arranged as follows: In Section II is given the short description of AC-KLT for color images; in Sections III and IV are correspondingly presented the RAC-KLT method and algorithm; in Section V the computational complexity of RAC-KLT is compared with that of AC-KLT; in Section VI are shown some experimental results; in Section VII are commented a part of the possible applications of the new algorithm, and Section VIII contains the conclusions.

Prof. D. Sc. PhD. R. K. Kountchev is with the Technical University of Sofia, Department of Radio Communications and Video Technologies, Bul. Kl. Ohridsky 8, Sofia 1000, Bulgaria (corresponding author, phone: +899924284) e-mail: rkountch@tu-sofia.bg).

Dr. R. A. Kountcheva is with TK Engineering, Sofia, Bulgaria (e-mail: kountcheva_r@yahoo.com).

II. ADAPTIVE COLOR KLT FOR THE IMAGE RGB COMPONENTS

Here follows the brief mathematical description of the RGB color space transform of the color image by using the AC-KLT, in accordance with [15]. The transform has two basic forms: Arithmetic and Trigonometric.

A. Arithmetic form of AC-KLT

Direct AC-KLT for the R,G,B components of the image of S pixels and of size $m \times n = S$:

$$\vec{L}_s = [\Phi](\vec{C}_s - \vec{m}) \text{ or } \vec{L}_s = [\Phi]\vec{X}_s \text{ for } s=1,2,\dots,S. \quad (1)$$

Here $\vec{C}_s = [R_s, G_s, B_s]^T$ is the color vector which represents the processed pixel s from the image of S pixels;

$\vec{L}_s = [L_{1s}, L_{2s}, L_{3s}]^T$ - the transformed color vector of the pixel s;

$\vec{m} = [E(R_s), E(G_s), E(B_s)]^T$ - the mean color vector,

where $\bar{x} = E(x_s) = (1/S) \sum_{s=1}^S x_s$ is the averaging operator for x_s in respect to s;

$\vec{X}_s = \vec{C}_s - \vec{m} = [x_{1s}, x_{2s}, x_{3s}]^T$ - the modified color vector s, for which $E(\vec{X}_s) = 0$;

$[\Phi]^T = [\vec{\Phi}_1, \vec{\Phi}_2, \vec{\Phi}_3]$ - the transposed matrix of size 3×3 used for the adaptive color KLT;

$\vec{\Phi}_k = [\Phi_{1k}, \Phi_{2k}, \Phi_{3k}]^T$ when $k=1,2,3$ are the eigen vectors of the color covariance matrix defined on the basis of the modified vectors $\vec{X}_s = [x_{1s}, x_{2s}, x_{3s}]^T$:

$$[K_c] = E(\vec{X}_s \vec{X}_s^T) = \frac{1}{S-1} \sum_{s=1}^S \vec{X}_s \vec{X}_s^T. \quad (2)$$

The elements k_{ij} of this matrix are symmetric in respect to its main diagonal, and it is represented as:

$$[K_c] = \begin{bmatrix} k_{11} & k_{12} & k_{13} \\ k_{21} & k_{22} & k_{23} \\ k_{31} & k_{32} & k_{33} \end{bmatrix} = \begin{bmatrix} k_1 & k_4 & k_5 \\ k_4 & k_2 & k_6 \\ k_5 & k_6 & k_3 \end{bmatrix}. \quad (3)$$

In the relation above are used the substitutions: $k_1 = k_{11}$, $k_2 = k_{22}$, $k_3 = k_{33}$, $k_4 = k_{12} = k_{21}$, $k_5 = k_{13} = k_{31}$, $k_6 = k_{23} = k_{32}$. The elements $k_1 \div k_6$ of the covariance matrix are calculated from the relations:

$$k_1 = E(R_s^2) - (\bar{R})^2, \quad k_2 = E(G_s^2) - (\bar{G})^2, \quad k_3 = E(B_s^2) - (\bar{B})^2; \quad (4)$$

$$k_4 = E(R_s G_s) - (\bar{R})(\bar{G}),$$

$$k_5 = E(R_s B_s) - (\bar{R})(\bar{B}), \quad (5)$$

$$k_6 = E(G_s B_s) - (\bar{G})(\bar{B}).$$

The eigenvectors $\vec{\Phi}_k$ of the matrix $[K_c]$ are the solution of the set of equations:

$$[K_c] \vec{\Phi}_k = \lambda_k \vec{\Phi}_k \text{ and } \left| \vec{\Phi}_k \right|^2 = \sum_{i=1}^3 \Phi_{ki}^2 = 1 \text{ for } k=1,2,3. \quad (6)$$

The eigenvalues $\lambda_1, \lambda_2, \lambda_3$ of the matrix $[K_c]$ are the solution of its characteristic equation:

$$\det |k_{ij} - \lambda \delta_{ij}| = \lambda^3 + a\lambda^2 + b\lambda + c = 0, \quad (7)$$

where for $\delta_{ij} = \begin{cases} 1, & i=j, \\ 0, & i \neq j. \end{cases}$ is got:

$$a = -(k_1 + k_2 + k_3),$$

$$b = k_1 k_2 + k_1 k_3 + k_2 k_3 - (k_4^2 + k_5^2 + k_6^2), \quad (8)$$

$$c = k_1 k_6^2 + k_2 k_5^2 + k_3 k_4^2 - (k_1 k_2 k_3 + 2k_4 k_5 k_6),$$

The matrix $[K_c]$ is symmetrical and its eigenvalues are always real numbers. They can be defined using the Cardano relations for the "casus irreducibilis" (or the so-called "trigonometric solution"):

$$\lambda_1 = 2\sqrt{|p|/3} \cos(\varphi/3) - (a/3), \quad (9)$$

$$\lambda_{2,3} = -2\sqrt{|p|/3} \cos[(\varphi \mp \pi)/3] - (a/3).$$

For these eigenvalues are satisfied the relations:

$$\lambda_1 \geq \lambda_2 \geq \lambda_3 \geq 0 \text{ and } \lambda_1 + \lambda_2 + \lambda_3 = k_1 + k_2 + k_3.$$

In (9) are used the following quantities:

$$q = 2(a/3)^3 - (ab)/3 + c,$$

$$p = -(a^2/3) + b < 0, \quad (10)$$

$$\varphi = \arccos [-q/2 / \sqrt{(|p|/3)^3}].$$

The solution of the systems of equations (6) defines the elements Φ_{ik} of the matrix $[\Phi]$ when $i, k=1,2,3$, and the rows of the matrix comprise the eigen vectors $\vec{\Phi}_k$.

$$\Phi_{i1} = A_i/P_1, \quad \Phi_{i2} = B_i/P_1, \quad \Phi_{i3} = D_i/P_1 \text{ for } i=1,2,3, \quad (11)$$

where

$$A_i = (k_3 - \lambda_i)[k_5(k_2 - \lambda_i) - k_4 k_6], \quad (12)$$

$$B_i = (k_3 - \lambda_i)[k_6(k_1 - \lambda_i) - k_4 k_5],$$

$$D_i = k_6[2k_4 k_5 - k_6(k_1 - \lambda_i)] - k_5^2(k_2 - \lambda_i), \quad (13)$$

$$P_i = \sqrt{A_i^2 + B_i^2 + D_i^2}.$$

Then from (11) it follows that the direct AC-KLT could be represented as given below:

$$\begin{bmatrix} L_{1s} \\ L_{2s} \\ L_{3s} \end{bmatrix} = \begin{bmatrix} A_1/P_1 & B_1/P_1 & D_1/P_1 \\ A_2/P_2 & B_2/P_2 & D_2/P_2 \\ A_3/P_3 & B_3/P_3 & D_3/P_3 \end{bmatrix} \times \left(\begin{bmatrix} R_s \\ G_s \\ B_s \end{bmatrix} - \begin{bmatrix} E(R_s) \\ E(G_s) \\ E(B_s) \end{bmatrix} \right). \quad (14)$$

The inverse AC-KLT is defined by the relations:

$$\vec{C}_s = [\Phi]^T \vec{L}_s + \vec{m} \text{ or } \vec{X}_s = [\Phi]^T \vec{L}_s. \quad (15)$$

From (14) and (15) it follows that the inverse AC-KLT could be represented as:

$$\begin{bmatrix} R_s \\ G_s \\ B_s \end{bmatrix} = \begin{bmatrix} A_1/P_1 & A_2/P_2 & A_3/P_3 \\ B_1/P_1 & B_2/P_2 & B_3/P_3 \\ D_1/P_1 & D_2/P_2 & D_3/P_3 \end{bmatrix} \times \begin{bmatrix} L_{1s} \\ L_{2s} \\ L_{3s} \end{bmatrix} + \begin{bmatrix} E(R_s) \\ E(G_s) \\ E(B_s) \end{bmatrix}. \quad (16)$$

As a result of the direct AC-KLT, the energy of the first component (L_{1s}) of the transformed vector \vec{L}_s is maximum, while the second (L_{2s}) is much smaller, and the last (L_{3s}) is close to zero.

B. Trigonometric form of AC-KLT

The matrix $[\Phi]$ could be represented through the Euler rotation angles (α, β, γ) :

$$[\Phi] = \begin{bmatrix} \Phi_{11} & \Phi_{12} & \Phi_{13} \\ \Phi_{21} & \Phi_{22} & \Phi_{23} \\ \Phi_{31} & \Phi_{32} & \Phi_{33} \end{bmatrix} = \quad (17)$$

$$[\Phi_1(\alpha)][\Phi_2(\beta)][\Phi_3(\gamma)] = [\Phi(\alpha, \beta, \gamma)],$$

where the angles α, β, γ define the position of the transform coordinate axes L_1, L_2, L_3 in respect to the original RGB color space;

$$[\Phi_1(\alpha)] = \begin{bmatrix} \cos \alpha & -\sin \alpha & 0 \\ \sin \alpha & \cos \alpha & 0 \\ 0 & 0 & 1 \end{bmatrix};$$

$$[\Phi_2(\beta)] = \begin{bmatrix} \cos \beta & 0 & \sin \beta \\ 0 & 1 & 0 \\ -\sin \beta & 0 & \cos \beta \end{bmatrix}; \quad (18)$$

$$[\Phi_3(\gamma)] = \begin{bmatrix} \cos \gamma & -\sin \gamma & 0 \\ \sin \gamma & \cos \gamma & 0 \\ 0 & 0 & 1 \end{bmatrix}.$$

From (17) and (18) it follows that the elements of the matrix $[\Phi]$ are defined by the relations:

$$\Phi_{11} = \cos \alpha \cos \beta \cos \gamma - \sin \alpha \sin \gamma;$$

$$\Phi_{12} = -\cos \alpha \cos \beta \sin \gamma - \sin \alpha \cos \gamma; \quad \Phi_{13} = \cos \alpha \sin \beta; \quad (19)$$

$$\Phi_{21} = \sin \alpha \cos \beta \cos \gamma + \cos \alpha \sin \gamma;$$

$$\Phi_{22} = -\sin \alpha \cos \beta \sin \gamma + \cos \alpha \cos \gamma; \quad \Phi_{23} = \sin \alpha \sin \beta; \quad (20)$$

$$\Phi_{31} = -\sin \beta \cos \gamma; \quad \Phi_{32} = \sin \beta \sin \gamma; \quad \Phi_{33} = \cos \beta. \quad (21)$$

The matrix of the inverse AC-KLT in this case is defined by the relation:

$$[\Phi]^{-1} = [\Phi]^T = [\Phi_1(-\gamma)][\Phi_2(-\beta)][\Phi_3(-\alpha)]. \quad (22)$$

Hence, to define $[\Phi]^{-1}$ are needed the Euler angles α, β and γ only. These angles are calculated using the elements of the matrix $[\Phi]$:

$$\alpha = \arcsin(\Phi_{23} / \sqrt{1 - \Phi_{33}^2}) = \arcsin(D_2 P_3 / P_2 \sqrt{A_3^2 + B_3^2}); \quad (23)$$

$$\beta = \arccos(\Phi_{33}) = \arccos(D_3 / P_3); \quad (24)$$

$$\gamma = \arccos(\Phi_{32} / \sqrt{1 - \Phi_{33}^2}) = \arccos(B_3 / \sqrt{A_3^2 + B_3^2}). \quad (25)$$

The elements of the matrix $[\Phi]^{-1}$ are calculated by using the angles α, β, γ . As a result, to the decoder are transferred the values of angles α, β, γ only, instead of all 9 elements of the matrix $[\Phi]^{-1}$, i.e. the number of the needed coefficients is 3 times smaller.

III. RECURSIVE ADAPTIVE COLOR KLT METHOD FOR A SEQUENCE OF CORRELATED COLOR IMAGES

The method, called Recursive Adaptive Color KLT (RAC-KLT) is aimed at the processing of a sequence of correlated images separated into groups with fixed, or adaptively changing length. In the first case, the fixed length is defined on

the basis of the averaged range of the mutual correlation calculated for the images in the group. In the second case, the length is set in accordance with the value of the mutual correlation between the couples of neighbor images in the group, which should be higher than a pre-selected threshold. The method RAC-KLT is applied for the images from each group, got after separation into sub-groups with fixed, or adaptive changing length (number of images in the group). One example for a group of sequential video frames is shown on Fig. 1. The group is of fixed length of 8 images ($N=8$).

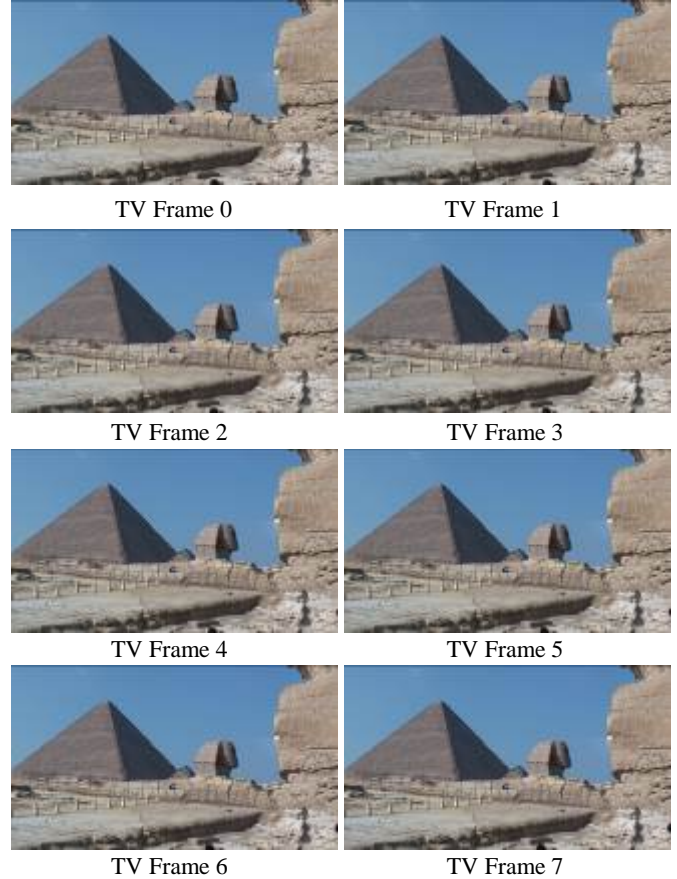


Fig. 1. A sequence of 8 TV frames, 25 fps. The images are of size 1920×1080 each, in format.bmp, 24 bpp

The processing of one group of images through RAC-KLT comprises the following basic operations:

- Recursive calculation of the color covariance matrix $[K_{c,t}]$ of the processed image with sequential number t , by using $[K_{c,t-1}]$, calculated for the preceding image, with number $(t-1)$:

$$[K_{c,t}] = [K_{c,t-1}] + [\Delta K_{c,t}]. \quad (26)$$

where

$$[\Delta K_{c,t}] = \begin{bmatrix} \Delta k_{1,t} & \Delta k_{4,t} & \Delta k_{5,t} \\ \Delta k_{4,t} & \Delta k_{2,t} & \Delta k_{6,t} \\ \Delta k_{5,t} & \Delta k_{6,t} & \Delta k_{3,t} \end{bmatrix} = \begin{bmatrix} (k_{1,t} - k_{1,t-1}) & (k_{4,t} - k_{4,t-1}) & (k_{5,t} - k_{5,t-1}) \\ (k_{4,t} - k_{4,t-1}) & (k_{2,t} - k_{2,t-1}) & (k_{6,t} - k_{6,t-1}) \\ (k_{5,t} - k_{5,t-1}) & (k_{6,t} - k_{6,t-1}) & (k_{3,t} - k_{3,t-1}) \end{bmatrix}. \quad (27)$$

It is supposed here that in the related equations all quantities with index $(t-1)$ are already calculated for the previous image with sequential number $(t-1)$ and are stored in the dynamic buffer memory.

- Recursive calculation of the eigen vectors $\vec{\Phi}_{k,t}$ for $k = 1, 2, 3$:

$$\vec{\Phi}_{k,t} = \vec{\Phi}_{k,t-1} + \Delta\vec{\Phi}_{k,t}, \quad (28)$$

where each difference k^{th} eigen vector $\Delta\vec{\Phi}_{k,t} = \vec{\Phi}_{k,t} - \vec{\Phi}_{k,t-1}$ is the solution of the system of linear equations:

$$[\Delta K_{c,t}] \Delta\vec{\Phi}_{k,t} = \Delta\lambda_{k,t} \vec{\Phi}_{k,t} \text{ for } k=1,2,3. \quad (29)$$

The difference eigen values $\Delta\lambda_{k,t}$ of the matrix $[\Delta K_{c,t}]$ are defined by relations, similar to (9)-(10), and the matrix $[\Phi_t]$ - by relations, similar to (19)-(21). Each of the participating quantities should be assigned the index t .

- Recursive calculation of the angles $\alpha_t, \beta_t, \gamma_t$ for the processed image t :

$$\alpha_t = \alpha_{t-1} + \Delta\alpha_t, \quad \beta_t = \beta_{t-1} + \Delta\beta_t, \quad \gamma_t = \gamma_{t-1} + \Delta\gamma_t, \quad (30)$$

where the difference angles are defined by analogy with (23) - (25):

$$\begin{aligned} \Delta\alpha_t &= \arcsin(\Delta D_{2,t} \Delta P_{3,t} / \Delta P_{2,t} \sqrt{\Delta A_{3,t}^2 + \Delta B_{3,t}^2}), \\ \Delta\beta_t &= \arccos(\Delta D_{3,t} / \Delta P_{3,t}), \\ \Delta\gamma_t &= \arccos(\Delta B_{3,t} / \sqrt{\Delta A_{3,t}^2 + \Delta B_{3,t}^2}). \end{aligned} \quad (31)$$

- Calculation of the direct RAC-KLT for the vectors $\vec{X}_{s,t} = \vec{C}_{s,t} - \vec{m}_t$ in accordance with the relations:

$$\vec{L}_s = [\Phi(\alpha_t, \beta_t, \gamma_t)] \vec{X}_{s,t}, \text{ for } s=1, 2, \dots, S. \quad (32)$$

The matrix $[\Phi(\alpha_t, \beta_t, \gamma_t)]$ is defined by the relations (33) where in the last line the mutual correlation between the corresponding two sequential color images with sequential numbers (t) and ($t-1$) is close to 100 %. This permits the calculations needed for AC-KLT to be reduced many times, because the matrix $[\Phi_t]$ is not necessary to be calculated (instead, the already calculated matrix $[\Phi_{t-1}]$ is used).

$$\vec{L}_{s,t} = \begin{cases} [\Phi(\alpha_t, \beta_t, \gamma_t)] \vec{X}_{s,t}, & \text{if } \Delta\alpha_t \neq 0, \Delta\beta_t \neq 0, \Delta\gamma_t \neq 0; \\ [\Phi_1(\alpha_{t-1})][\Phi_2(\beta_t)][\Phi_3(\gamma_t)] \vec{X}_{s,t}, & \text{if } \Delta\alpha_t \approx 0, \Delta\beta_t \neq 0, \Delta\gamma_t \neq 0; \\ [\Phi_1(\alpha_t)][\Phi_2(\beta_{t-1})][\Phi_3(\gamma_t)] \vec{X}_{s,t}, & \text{if } \Delta\alpha_t \neq 0, \Delta\beta_t \approx 0, \Delta\gamma_t \neq 0; \\ [\Phi_1(\alpha_t)][\Phi_2(\beta_t)][\Phi_3(\gamma_{t-1})] \vec{X}_{s,t}, & \text{if } \Delta\alpha_t \neq 0, \Delta\beta_t \neq 0, \Delta\gamma_t \approx 0; \\ [\Phi_1(\alpha_{t-1})][\Phi_2(\beta_{t-1})][\Phi_3(\gamma_t)] \vec{X}_{s,t}, & \text{if } \Delta\alpha_t \approx 0, \Delta\beta_t \approx 0, \Delta\gamma_t \neq 0; \\ [\Phi_1(\alpha_{t-1})][\Phi_2(\beta_t)][\Phi_3(\gamma_{t-1})] \vec{X}_{s,t}, & \text{if } \Delta\alpha_t \approx 0, \Delta\beta_t \neq 0, \Delta\gamma_t \approx 0; \\ [\Phi_1(\alpha_t)][\Phi_2(\beta_{t-1})][\Phi_3(\gamma_{t-1})] \vec{X}_{s,t}, & \text{if } \Delta\alpha_t \neq 0, \Delta\beta_t \approx 0, \Delta\gamma_t \approx 0; \\ [\Phi_1(\alpha_{t-1})][\Phi_2(\beta_{t-1})][\Phi_3(\gamma_{t-1})] \vec{X}_{s,t}, & \text{if } \Delta\alpha_t \approx 0, \Delta\beta_t \approx 0, \Delta\gamma_t \approx 0; \end{cases} \quad (33)$$

- Calculation of the inverse RAC-KLT (IRAC-KLT) by analogy with (15):

$$\vec{X}_{s,t} = [\Phi_t]^{-1} \vec{L}_{s,t} = [\Phi_t]^{-1} \vec{L}_{s,t} \text{ or } \vec{C}_{s,t} = [\Phi_t]^{-1} \vec{L}_{s,t} + \vec{m}_t. \quad (34)$$

Here the inverse transform matrix $[\Phi_t]^{-1}$ and the vectors $\vec{L}_{s,t}, \vec{C}_{s,t}, \vec{m}_t$ are calculated recursively:

$$[\Phi_t]^{-1} = [\Phi_{t-1}]^{-1} + [\Delta\Phi_t]^{-1}, \quad (35)$$

$$\vec{L}_{s,t} = \vec{L}_{s,t-1} + \Delta\vec{L}_{s,t},$$

$$\vec{C}_{s,t} = \vec{C}_{s,t-1} + \Delta\vec{C}_{s,t}, \quad (36)$$

$$\vec{m}_t = \vec{m}_{t-1} + \Delta\vec{m}_t.$$

The difference matrix for the inverse transform $[\Delta\Phi_t]^{-1}$ is calculated by analogy with (22), using the inverse rotation angles $(-\Delta\gamma_t), (-\Delta\beta_t), (-\Delta\alpha_t)$.

IV. RAC-KLT ALGORITHM FOR A GROUP OF COLOR IMAGES

On the basis of the already presented method was developed the algorithm RAC-KLT for processing a group of N images, where $t = 0, 1, \dots, N-1$ is the number of the currently processed image.

A. Algorithm for direct RAC-KLT

For the first image with components $[R_0], [G_0], [B_0]$ in the group (image with number $t=0$) is executed the algorithm initialization, which comprises the following steps:

Step 1. Calculation of the elements $k_{l,0} \div k_{6,0}$ of the initial color covariance matrix $[K_{c,0}]$, in correspondence with (4)-(5);

Step 2. Calculation of the parameters $a_0, b_0, c_0, q_0, \varphi_0, \lambda_{1,0}, \lambda_{2,0}, \lambda_{3,0}, A_{3,0}, B_{3,0}, D_{2,0}, P_{2,0}, P_{3,0}$ - in correspondence with (8) - (13);

Step 3. Calculation of the trigonometric functions $\sin(\alpha_0), \cos(\alpha_0), \sin(\beta_0), \cos(\beta_0), \sin(\gamma_0), \cos(\gamma_0)$ for the angles $\alpha_0, \beta_0, \gamma_0$ in correspondence c (23) - (25);

Step 4. Calculation of the initial AC-KLT matrix $[\Phi_0]$ as a product of the corresponding initial rotation matrices $[\Phi_1(\alpha_0)], [\Phi_1(\beta_0)], [\Phi_1(\gamma_0)]$, defined in accordance with the relations (17) - (21);

Step 5. Calculation of $\vec{m}_0 = [E(R_{s,0}), E(G_{s,0}), E(B_{s,0})]^T$ - the initial mean color vector;

Step 6. Calculation of the transformed color vectors $\vec{L}_{s,0}$ for the image $t=0$ and $s=1, 2, \dots, S$ in correspondence c (1).

For the next images in the group ($t=t+1$ for $t \leq N-1$) are executed the steps given below (similar to these for the image with number $t=0$):

Step 7. Calculation of the rotation angles $\alpha_t, \beta_t, \gamma_t$ for the image $t=t+1$ using relations, similar to these from Step 3, where the index 0 is replaced by t .

Step 8. Calculation of the difference rotation angles for the image t :

$$\Delta\alpha_t = \alpha_t - \alpha_{t-1}; \quad \Delta\beta_t = \beta_t - \beta_{t-1}; \quad \Delta\gamma_t = \gamma_t - \gamma_{t-1}. \quad (37)$$

Step 9. Calculation of the approximated angles $\hat{\alpha}_t, \hat{\beta}_t, \hat{\gamma}_t$ for the image t :

$$\hat{\alpha}_t = \begin{cases} \hat{\alpha}_{t-1}, & \text{if } |\Delta\alpha_t| < \delta; \\ \hat{\alpha}_{t-1} + \Delta\alpha_t & \text{- in other cases,} \end{cases} \quad (38)$$

$$\hat{\beta}_t = \begin{cases} \hat{\beta}_{t-1}, & \text{if } |\Delta\beta_t| < \delta; \\ \hat{\beta}_{t-1} + \Delta\beta_t & \text{- in other cases,} \end{cases} \quad (39)$$

$$\hat{\gamma}_t = \begin{cases} \hat{\gamma}_{t-1}, & \text{if } |\Delta\gamma_t| < \delta; \\ \hat{\gamma}_{t-1} + \Delta\gamma_t & \text{- in other cases,} \end{cases} \quad (40)$$

In the relations above \hat{x} means the approximation of x , and δ is a preset threshold (a small number, for example, in the range 0,01-0,05), which defines the accuracy of the restored color vectors after the inverse RAC-KLT, and the volume of data which represents the difference angles.

Step 10. The values of functions $\sin \hat{\alpha}_t$, $\cos \hat{\alpha}_t$, $\sin \hat{\beta}_t$, $\cos \hat{\beta}_t$, $\sin \hat{\gamma}_t$ and $\cos \hat{\gamma}_t$ are set from the pre-calculated tables. After that, the matrix $[\Phi_t(\hat{\alpha}_t, \hat{\beta}_t, \hat{\gamma}_t)]$ is calculated as the product of the three matrices $[\Phi_1(\hat{\alpha}_t)]$, $[\Phi_2(\hat{\beta}_t)]$ and $[\Phi_3(\hat{\gamma}_t)]$ in correspondence with Step 4, where the index 0 is replaced by t .

Step 11. Calculation of the mean color vector \bar{m}_t for the image t , in correspondence with Step 5, where the index 0 was replaced by t , and the vectors are $\bar{X}_{s,t} = \bar{C}_{s,t} - \bar{m}_t$;

Step 12. Calculation of the restored vectors $\bar{L}_{s,t}$ for $s=1,2,\dots,S$ on the basis of (38) - (40) and the relations in (41):

$$\bar{L}_{s,t} = \begin{cases} [\Phi_1(\hat{\alpha}_t)][\Phi_2(\hat{\beta}_t)][\Phi_3(\hat{\gamma}_t)]\bar{X}_{s,t}, & \text{if } |\Delta\hat{\alpha}_t| \geq \delta, |\Delta\hat{\beta}_t| \geq \delta, |\Delta\hat{\gamma}_t| \geq \delta; \\ [\Phi_1(\hat{\alpha}_{t-1})][\Phi_2(\hat{\beta}_t)][\Phi_3(\hat{\gamma}_t)]\bar{X}_{s,t}, & \text{if } |\Delta\hat{\alpha}_t| < \delta, |\Delta\hat{\beta}_t| \geq \delta, |\Delta\hat{\gamma}_t| \geq \delta; \\ [\Phi_1(\hat{\alpha}_t)][\Phi_2(\hat{\beta}_{t-1})][\Phi_3(\hat{\gamma}_t)]\bar{X}_{s,t}, & \text{if } |\Delta\hat{\alpha}_t| \geq \delta, |\Delta\hat{\beta}_t| < \delta, |\Delta\hat{\gamma}_t| \geq \delta; \\ [\Phi_1(\hat{\alpha}_t)][\Phi_2(\hat{\beta}_t)][\Phi_3(\hat{\gamma}_{t-1})]\bar{X}_{s,t}, & \text{if } |\Delta\hat{\alpha}_t| \geq \delta, |\Delta\hat{\beta}_t| \geq \delta, |\Delta\hat{\gamma}_t| < \delta; \\ [\Phi_1(\hat{\alpha}_{t-1})][\Phi_2(\hat{\beta}_{t-1})][\Phi_3(\hat{\gamma}_t)]\bar{X}_{s,t}, & \text{if } |\Delta\hat{\alpha}_t| < \delta, |\Delta\hat{\beta}_t| < \delta, |\Delta\hat{\gamma}_t| \geq \delta; \\ [\Phi_1(\hat{\alpha}_{t-1})][\Phi_2(\hat{\beta}_t)][\Phi_3(\hat{\gamma}_{t-1})]\bar{X}_{s,t}, & \text{if } |\Delta\hat{\alpha}_t| < \delta, |\Delta\hat{\beta}_t| \geq \delta, |\Delta\hat{\gamma}_t| < \delta; \\ [\Phi_1(\hat{\alpha}_t)][\Phi_2(\hat{\beta}_{t-1})][\Phi_3(\hat{\gamma}_{t-1})]\bar{X}_{s,t}, & \text{if } |\Delta\hat{\alpha}_t| \geq \delta, |\Delta\hat{\beta}_t| < \delta, |\Delta\hat{\gamma}_t| < \delta; \\ [\Phi_1(\hat{\alpha}_{t-1})][\Phi_2(\hat{\beta}_{t-1})][\Phi_3(\hat{\gamma}_{t-1})]\bar{X}_{s,t}, & \text{if } |\Delta\hat{\alpha}_t| < \delta, |\Delta\hat{\beta}_t| < \delta, |\Delta\hat{\gamma}_t| < \delta; \end{cases} \quad (41)$$

Step 13. Calculation of the modified angles $\Delta\alpha_t^*$, $\Delta\beta_t^*$, $\Delta\gamma_t^*$ satisfying the rules:

$$\Delta\alpha_t^* = \begin{cases} 0, & \text{if } |\Delta\alpha_t| < \delta; \\ \Delta\alpha_t & \text{- in other cases,} \end{cases} \quad (42)$$

$$\Delta\beta_t^* = \begin{cases} 0, & \text{if } |\Delta\beta_t| < \delta; \\ \Delta\beta_t & \text{- in other cases,} \end{cases} \quad (43)$$

$$\Delta\gamma_t^* = \begin{cases} 0, & \text{if } |\Delta\gamma_t| < \delta; \\ \Delta\gamma_t & \text{- in other cases.} \end{cases} \quad (44)$$

Step 14. Calculation of the difference vectors:

$$\Delta\bar{L}_{s,t} = \bar{L}_{s,t} - \bar{L}_{s,t-1}, \quad \Delta\bar{m}_t = \bar{m}_t - \bar{m}_{t-1}. \quad (46)$$

Step 15. Calculation of the quantized difference vectors $\bar{L}_{s,t}^* = [L_{1,s,t}^*, L_{2,s,t}^*, L_{3,s,t}^*]^T$:

$$\Delta\hat{L}_{1,s,t}^* = \begin{cases} 0, & \text{if } |\Delta\hat{L}_{1,s,t}| < \theta_1; \\ \Delta\hat{L}_{1,s,t} & \text{- in all other cases,} \end{cases} \quad (47)$$

$$\Delta\hat{L}_{2,s,t}^* = \begin{cases} 0, & \text{if } |\Delta\hat{L}_{2,s,t}| < \theta_2; \\ \Delta\hat{L}_{2,s,t} & \text{- in all other cases,} \end{cases} \quad (48)$$

$$\Delta\hat{L}_{3,s,t}^* = \begin{cases} 0, & \text{if } |\Delta\hat{L}_{3,s,t}| < \theta_3; \\ \Delta\hat{L}_{3,s,t} & \text{- in all other cases,} \end{cases} \quad (50)$$

where θ_1 , θ_2 , θ_3 are thresholds defined in accordance with the mean noise value in the corresponding component of the vector $\Delta\bar{L}_{s,t}$. In the general case, each component $\Delta\hat{L}_{i,s,t}$ has to be quantized in corresponding nonlinear scale $Q_i(\Delta\hat{L}_{i,s,t})$, whose levels are harmonized with the image histogram.

When t gets the value $t=N$, the execution of the direct RAC-KLT for the group of images is finished. As a result, the values of the vectors' components of $\bar{L}_{s,0}$, \bar{m}_0 , $\Delta\bar{L}_{s,t}$, $\Delta\bar{m}_t$ and of the angles $\alpha_0, \beta_0, \gamma_0, \Delta\alpha_t^*, \Delta\beta_t^*, \Delta\gamma_t^*$ for $t=0,1,2,\dots,N-1$ and $s=1,2,\dots,S$, are got. After that they could be efficiently coded using various methods, selected in accordance with the application of the algorithm RAC-KLT.

B. Algorithm for inverse RAC-KLT

The input parameters, needed for the inverse RAC-KLT are:

- the initial angles $\alpha_0, \beta_0, \gamma_0$ and the components of the vectors $\bar{L}_{s,0}$ and \bar{m}_0 for the image with group number $t=0$, when $s=1,2,\dots,S$;

- the difference angles $\Delta\alpha_t^*, \Delta\beta_t^*, \Delta\gamma_t^*$ and the components of the vectors $\Delta\bar{L}_{s,t}$ and $\Delta\bar{m}_t$ for each image with number $t=1,2,\dots,N-1$, for $s=1,2,\dots,S$.

For the first image (with number $t=0$) the inverse RAC-KLT comprises the following steps:

Step 1. Calculation of the matrix $[\Delta\Phi_0]$ on the basis of the values of $\alpha_0, \beta_0, \gamma_0$ in correspondence with Step 4 of the algorithm for direct RAC-KLT;

Step 2. Calculation of the restored initial color vectors $\bar{C}_{s,0}$ for $s=1,2,\dots,S$ through the inverse RAC-KLT in correspondence with (15), where is added the index 0;

For each of the next images with number $t=t+1$ when $t \leq N-1$, the inverse RAC-KLT comprises the following steps:

Step 3. Calculation of the difference matrix $[\Delta\Phi_t]$ based on the values of $\Delta\alpha_t^*, \Delta\beta_t^*, \Delta\gamma_t^*$ in correspondence with the relations below.

$$[\Delta\Phi_t] = \begin{cases} [\Phi_1(\Delta\alpha_{t-1})][\Phi_2(\Delta\beta_t)][\Phi_3(\Delta\gamma_t)], & \text{if } \Delta\alpha_t^*=0, \Delta\beta_t^*\neq 0, \Delta\gamma_t^*\neq 0; \\ [\Phi_1(\Delta\alpha_{t-1})][\Phi_2(\Delta\beta_{t-1})][\Phi_3(\Delta\gamma_t)], & \text{if } \Delta\alpha_t^*\neq 0, \Delta\beta_t^*=0, \Delta\gamma_t^*\neq 0; \\ [\Phi_1(\Delta\alpha_{t-1})][\Phi_2(\Delta\beta_t)][\Phi_3(\Delta\gamma_{t-1})], & \text{if } \Delta\alpha_t^*=0, \Delta\beta_t^*\neq 0, \Delta\gamma_t^*=0; \\ [\Phi_1(\Delta\alpha_{t-1})][\Phi_2(\Delta\beta_{t-1})][\Phi_3(\Delta\gamma_t)], & \text{if } \Delta\alpha_t^*=0, \Delta\beta_t^*=0, \Delta\gamma_t^*\neq 0; \\ [\Phi_1(\Delta\alpha_{t-1})][\Phi_2(\Delta\beta_t)][\Phi_3(\Delta\gamma_{t-1})], & \text{if } \Delta\alpha_t^*\neq 0, \Delta\beta_t^*\neq 0, \Delta\gamma_t^*=0; \\ [\Phi_1(\Delta\alpha_t)][\Phi_2(\Delta\beta_{t-1})][\Phi_3(\Delta\gamma_{t-1})], & \text{if } \Delta\alpha_t^*\neq 0, \Delta\beta_t^*=0, \Delta\gamma_t^*=0; \\ [\Phi_1(\Delta\alpha_t)][\Phi_2(\Delta\beta_t)][\Phi_3(\Delta\gamma_t)], & \text{if } \Delta\alpha_t^*\neq 0, \Delta\beta_t^*\neq 0, \Delta\gamma_t^*\neq 0; \\ [\Phi_1(\Delta\alpha_{t-1})][\Phi_2(\Delta\beta_{t-1})][\Phi_3(\Delta\gamma_{t-1})], & \text{if } \Delta\alpha_t^*=0, \Delta\beta_t^*=0, \Delta\gamma_t^*=0. \end{cases} \quad (51)$$

Step 4. Calculation of the matrix $[\Phi_t]^T$ for the inverse RAC-KLT of the image t:

$$[\Phi_t]^T = [\Phi_{t-1}]^T + [\Delta\Phi_t]^T. \quad (52)$$

Step 5. Dequantization of the components $\Delta\hat{L}'_{i,s,t} = Q_i^{-1}(\Delta\hat{L}_{i,s,t})$ of the vectors $\vec{\Delta\hat{L}}'_{s,t} = [\Delta\hat{L}'_{1,s,t}, \Delta\hat{L}'_{2,s,t}, \Delta\hat{L}'_{3,s,t}]^T$ and calculation of the corresponding vectors $\vec{L}'_{s,t}$ and \vec{m}_t for the image t:

$$\vec{L}'_{r,t} = \vec{L}'_{r,t-1} + \Delta\hat{L}'_{r,t}, \quad \vec{m}_t = \vec{m}_{t-1} + \Delta\vec{m}_t. \quad (53)$$

Step 6. Restoration of the color vectors $\vec{C}'_{s,t}$ through the inverse AC-KLT:

$$\vec{C}'_{s,t} = [\Phi_t]^T \vec{L}'_{s,t} + \vec{m}_t \quad \text{for } s=1,2,\dots,S. \quad (54)$$

The execution of the inverse RAC-KLT stops when $t=N$ is satisfied.

The difference (error) between the restored vectors $\vec{C}'_{s,t}$ and the originals $\vec{C}_{s,t}$ is defined by the thresholds $\delta, \theta_1, \theta_2, \theta_3$ and the quantization scales $Q_i(\cdot)$ used for the calculation of the components of the difference vectors $\vec{\Delta\hat{L}}'_{s,t}$.

The presented algorithm RAC-KLT is asymmetric, because the number of calculations needed for the inverse transform is much lower than that for the direct.

V. EVALUATION OF RAC-KLT EFFICIENCY

The efficiency of RAC-KLT for a sequence of correlated color images is evaluated here through its comparison with AC-KLT. For this are used the number of parameters needed for the inverse transform, and the computational complexity of both algorithms.

A. Parameters calculated by direct AC-KLT and RAC-KLT

To execute the inverse color transform for each pixel s of the processed image from the sequence, should be known the values of the following parameters:

- for the AC-KLT - the parameters $\vec{L}_s, \vec{m}, \alpha, \beta, \gamma$, which are represented by $3(S+2)N$ numbers in total (S is the number of pixels in the single image, N - the number of the images in the sequence);

- for the RAC-KLT of the initial image with sequential number $t=0$ - the parameters $\vec{L}_{s,0}, \vec{m}_0, \alpha_0, \beta_0, \gamma_0$. For each of the next images in the sequence with number $t=1,2,\dots,N-1$ - the parameters $\vec{\Delta\hat{L}}'_{s,t}, \Delta\vec{m}_t, \Delta\hat{\alpha}_t, \Delta\hat{\beta}_t, \Delta\hat{\gamma}_t$, which for the whole group are represented by $3(S+2)+3(S+2)(N-1)=3(S+2)N$ numbers in total.

Hence, there is no difference between both algorithms in respect of the needed color parameters number. However, due to high mutual correlation between the neighbor images in the group, the values of large number of the direct RAC-KLT parameters are close, or equal to zero, while this number is much lower for the direct AC-KLT, because they have no relation with the mutual correlation. This is the main difference between RAC-KLT and AC-KLT.

B. Computational complexity of algorithms AC-KLT and RAC-KLT

The computational complexity of both algorithms could be evaluated on the basis of the computational operations (additions and multiplications) needed for their execution. Here follow the generalized data, got as a result of the analysis of the operations for direct and inverse color transform for a group of N images, S pixels each. The number of operations is:

- for the direct AC-KLT:

$$(37S+124)N \approx 37SN; \quad (55)$$

- for the RAC-KLT the calculation of the first image in the group needs $37S+124$ operations, and for the remaining images in the group the needed number of operations is $(37S+129)(N-1)$. In total, the needed operations for RAC-KLT are:

$$37S+124+(37S+129)(N-1) \approx 37SN; \quad (56)$$

Accordingly,

$$\text{- for the inverse AC-KLT: } (15S+23)N \approx 15SN; \quad (57)$$

$$\text{- for the inverse RAC-KLT: } (15S+47)N - 24 \approx 15SN. \quad (58)$$

Hence, the computational complexity of both algorithms is practically same.

The main advantage of RAC-KLT towards AC-KLT is the ability to achieve higher reduction of the color parameters data. As a result of the correlation between the couples of sequential images, the values of the difference angles $\Delta\alpha_t, \Delta\beta_t, \Delta\gamma_t$ and of the components of the difference vectors $\vec{\Delta\hat{L}}'_{s,t}$ for significant number of pixels in each image are close, or equal to zero. In this case, the use of various existing methods for lossless or visually lossless coding methods permits high reduction of the volume of the color components data, which should be transferred to the decoder. However, for the execution of the algorithm RAC-KLT is necessary to use larger memory volume to store the color data for the previous image in the group with number $(t-1)$. This problems could be considered easily solved because of the fast development of contemporary computer technologies.

The choice of the values for the thresholds δ and $\theta_1, \theta_2, \theta_3$ (the quantization scales $Q_i(\cdot)$, resp.) influences the restoration accuracy of the color vectors in the group for all images except the initial one, and also on the needed volume of data that represent the color parameters of the images. For lower

threshold values the accuracy of the restored color vectors is higher, but together with it grows up the needed volume of the color data, and vice versa. This is why these values should be selected depending on the application of RAC-KLT.

VI. EXPERIMENTAL RESULTS

Here are presented some experimental results of the comparison of the algorithm AC-KLT (abbreviated as ACT) and the standard deterministic color transform for static images, YCrCb [16,17,18]. For the experiments were used 3 sets of images of different size – the “Kodak image set“ of size 512×768 or 768×512, plus images “Lena” (512×512) and “Barbara” (640×512) - 26 images in total ; the “cgraph image set“ which comprises 10 computer generated images of size 1024×768, and the “natural image set“ which comprises 10 images of size 1920×1024 pixels. All images were in the format .bmp, 24 bpp. Example groups from the three test sets are shown on Fig. 2. For the elements of the first component [L₁] of ACT was used adaptive scalar quantization (ASQ) and the elements were represented as 8-bit numbers. On Fig. 3 are shown the results for the comparison of the PSNR (Peak Signal to Noise Ratio) in dB for all three image sets, generalized in Table 1. They show that the mean increase for the ACT compared to YCrCb is 2 dB, and for its next version, the Enhanced ACT (EACT) [18], based on histogram matching of the color components, the PSNR is up to 5 dB higher.

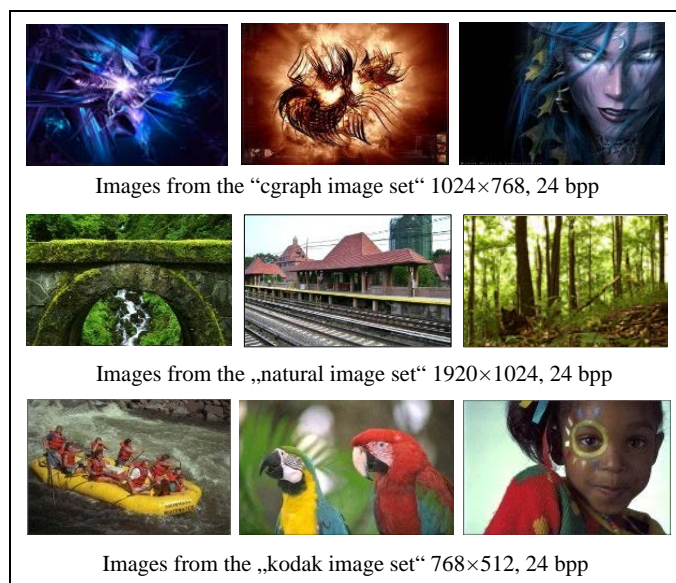


Fig. 2. Example images from 3 test image sets

Table1

Image set	YCrCb Mean PSNR [dB]	ACT Mean PSNR [dB]	EACT Mean PSNR [dB]
Kodak+2	46.57	48.44	50.79
Cgraph	46.12	48.97	51.24
Natural HD	46.01	48.59	50.17

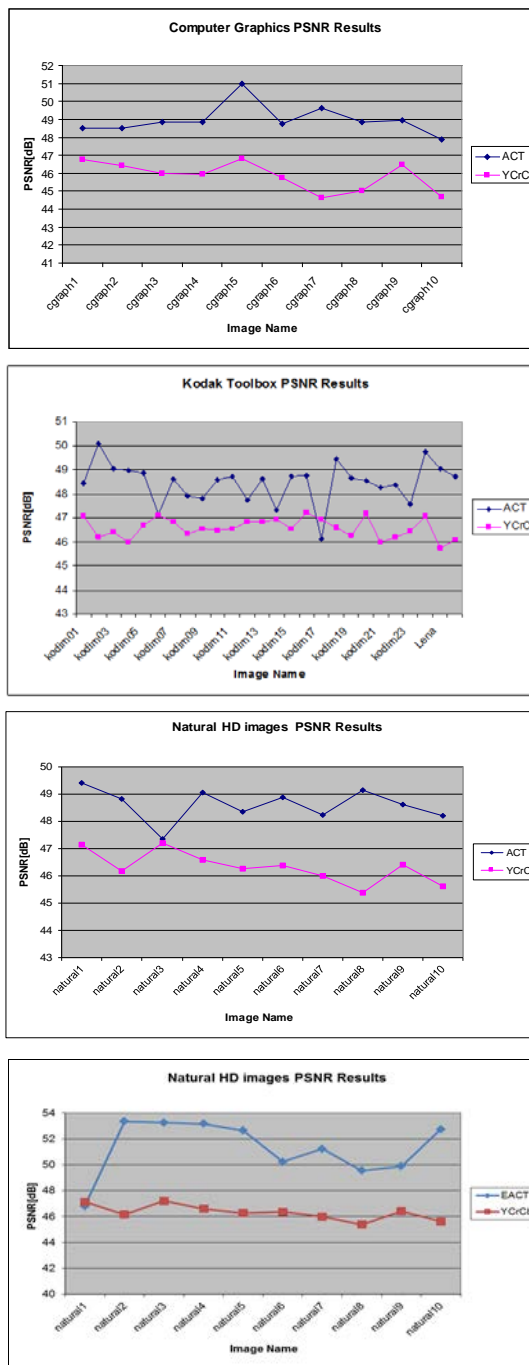


Fig 3. Results for the comparison of PSNR between ACT and EACT towards YCrCb

The comparison for the algorithms ACT and YCrCb about the power distribution of the three components [L₁],[L₂],[L₃] and [Y],[Cr],[Cb] for the group of 10 natural test images are shown on Fig. 4. They indicate the higher power concentration on the first component [L₁] and the monotonous decrease in the next two components [L₂] and [L₃], compared to the power distribution for the component [Y] and the next components, [Cr] and [Cb]. Besides, in the second case, for some images could be easily noticed the higher power concentration in the third component [Cb] than in the second, [Cr]. The results confirm the higher efficiency of ACT for all test images.

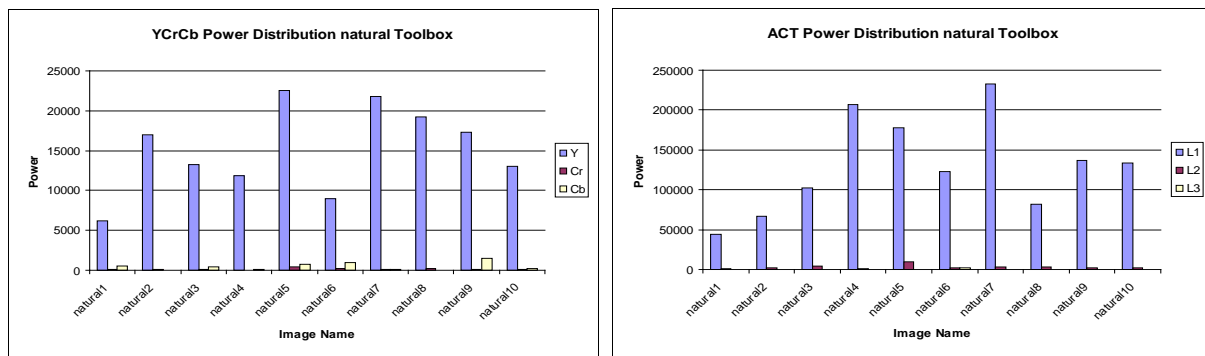


Fig. 4. Results for the comparison of the power distribution of the three color components for YCrCb and ACT

An example, illustrating the transforms YCrCb and ACT of the RGB image “Lena” and the corresponding three components [Y],[Cr],[Cb] and [L₁],[L₂],[L₃] is shown on Fig. 5. The obtained results confirm the conclusions about the

components power distribution for both transforms. Besides, this distribution is decreasing monotonously only for ACT.

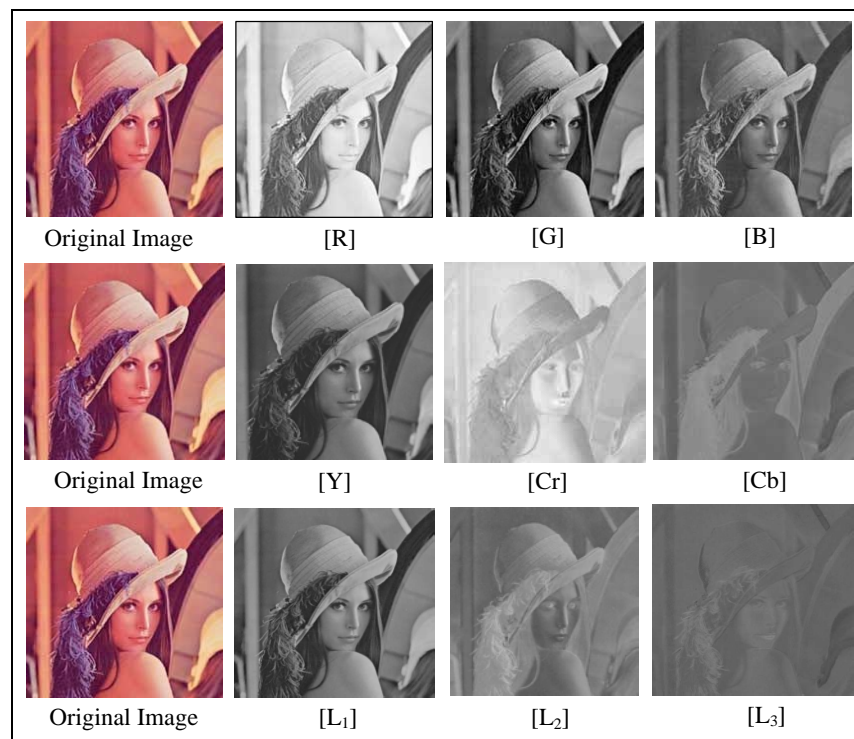


Fig. 5. Comparison of the RGB transform components obtained for YCrCb and ACT for the test image “Lena”

Some results about the application of algorithms AC-KLT and RAC-KLT are shown on Fig. 6. For the processing of the difference components ΔPC_1 for this sequence was used threshold value $\theta_1 = 16$. The differences obtained after the threshold transform are noted as $\text{thr}\Delta PC_1$. The difference frames that represent the components ΔPC_1 and $\text{thr}\Delta PC_1$ are given in second and third columns of Fig. 6, correspondingly. For better visualization these pictures are with enhanced contrast.

The opportunities for lossless compression of the input and output (transformed) sequence of TV frames were also investigated. The results obtained for the compression of the components $PC_1(t)$ of frames with sequential number $t=0,1,\dots,7$

when the standard JPEG 2000-LS for lossless compression was used, are given in Table 2.

On the basis of the averaged values from Table 2 were calculated the compression coefficients and relations, given below:

- *Mean compression coefficients CR_i , for $i=1,2,3,4$:*
 $\text{Mean}CR_1 = \text{Mean}[PC_1(\text{bmp})/PC_1(\text{jp2})] = 2.94$;
 $\text{Mean}CR_2 = \text{Mean}[PC_1(\text{bmp})/\Delta PC_1(\text{jp2})] = 3.36$;
 $\text{Mean}CR_3 = \text{Mean}[PC_1(\text{bmp})/\text{thr}\Delta PC_1(\text{jp2})] = 19.45$;
 $\text{Mean}CR_4 = \text{Mean}[\Delta PC_1(\text{jp2})/\text{thr}\Delta PC_1(\text{jp2})] = 5.79$.
- *Relations between the calculated compression coefficients:*
 $\text{Mean}(CR_2/CR_1) = 1.19$ - i.e., 19 % higher mean compression for $\Delta PC_1(\text{jp2})$ towards $PC_1(\text{jp2})$;

Mean $(CR_3/CR_1)=39.06$ - i.e., 39.06 times higher mean compression for $Thr\Delta PC_1(jp2)$ towards $PC_1(jp2)$;
 Mean $(CR_3/CR_2)=32.82$ - i.e., 32.82 times higher mean compression for $Thr\Delta PC_1(jp2)$ towards $\Delta PC_1(jp2)$;
 Mean $(CR_3/CR_4)=4.23$ - i.e., 4.23 times higher mean compression for $\Delta PC_1(jp2)$ towards $PC_1(bmp)$.

The presented results show that after applying the RAC-KLT on the non-compressed (bmp) frames, their first principal components PC_1 have average compression of 19.45. When AC-KLT used for same frames, compression ratio of 2.94 was obtained. For same example, the compression of PC_1 for RAC-KLT is 6.61 times higher than that for AC-KLT.

As it was shown, the power of the next components (PC_2 and PC_3) is much lower than that of PC_1 , and their RAC-KLT compression compared to AC-KLT grows faster, getting highest values for PC_3 (these results are not given here).

This analysis illustrates the higher efficiency of RAC-KLT compared to AC-KLT in respect of compression ratio for the investigated TV sequence. In future the algorithm RAC-KLT will be investigated experimentally in various application areas aiming at its parameters optimization for each specific case.

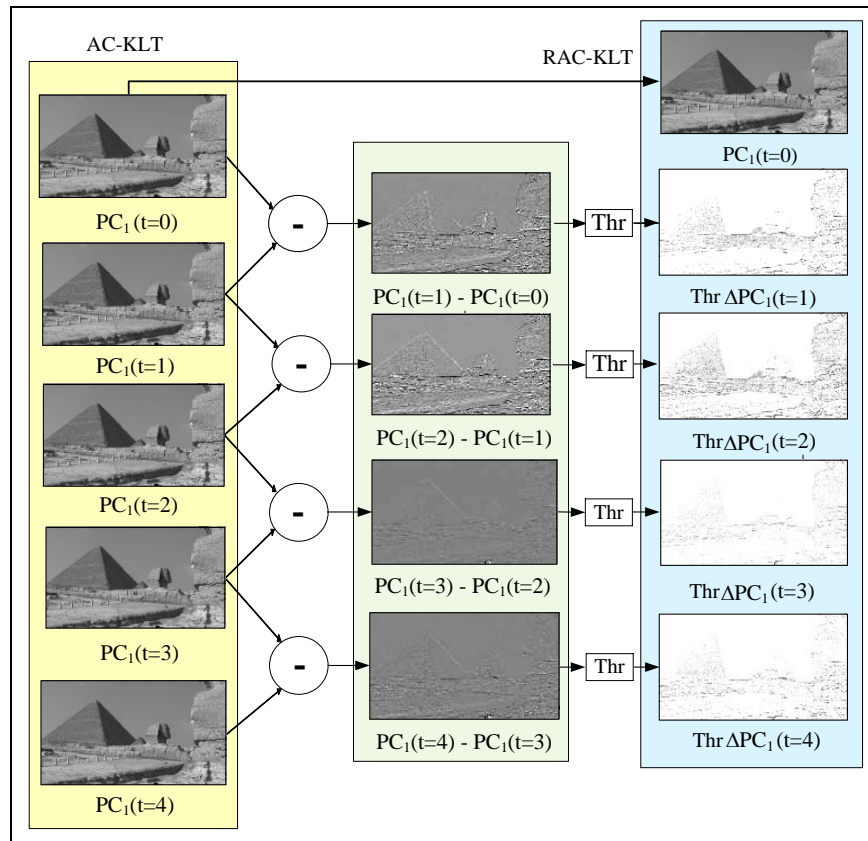


Fig. 6. Example for the application of algorithms AC-KLT and RAC-KLT concerning the first principal component PC_1 of the TV frames 0,1,2,3,4 from the sequence shown on Fig. 1

Table 2. Compression results for the PC_1 components of the frames from Fig. 1, through the standard JP2-LS

Number t of $PC_1(t)$	PC_1 (bmp) 1920×1080 8 bpp, KB	PC_1 (jp2) KB	$\Delta PC_1 = [PC_1(t) - PC_1(t-1)]$ (jp2), KB	$Thr\Delta PC_1 = Thr[PC_1(t) - PC_1(t-1)]$ (jp2), KB	$CR_1 = PC_1(bmp) / PC_1(jp2)$	$CR_2 = PC_1(bmp) / \Delta PC_1(jp2)$	$CR_3 = PC_1(bmp) / Thr \Delta PC_1(jp2)$	$CR_4 = \Delta PC_1(Jp2) / Thr \Delta PC_1(jp2)$
0	1970	684	(0) 684	(0) 684	2.88	2.88	2.88	1
1	1970	694	(1-0) 760	(1-0) 29.40	2.83	2.59	67.00	2.71
2	1970	652	(2-1) 757	(2-1) 30.80	3.02	2.60	51.84	19.93
3	1970	669	(3-2) 504	(3-2) 12.30	2.94	3.91	160.16	40.96
4	1970	654	(4-3) 547	(4-3) 16.20	3.01	3.60	121.60	33.77
5	1970	664	(5-4) 473	(5-4) 10.20	2.96	4.16	193.14	42.26
6	1970	651	(6-5) 431	(6-5) 9.31	3.02	4.57	211.60	46.30
7	1970	693	(7-6) 536	(7-6) 17.80	2.84	3.67	110.67	30.15
Mean	1970	670.12	586.5	101.25	2.94 1	3.50 2	114.86 3	27.13 4

VII. APPLICATION AREAS FOR RAC-KLT

On the basis of the efficiency evaluation of RAC-KLT used for the representation of the color components for a group of correlated images, here are defined the main future application areas:

- coding of video sequences got from stationary TV cameras used in the surveillance systems;
- search of closest images in databases containing the information got from surveillance TV cameras;
- segmentation and object recognition based on the color information in a group of images, etc.

In general, RAC-KLT could be also used in the digital TV systems, but in this case the methods for movement compensation should be added to the processing and calculation of the difference color vectors for each pixel and of the difference rotation angles for each frame, to overcome the problems related to the movement of the objects and the background. For real-time applications of RAC-KLT should be developed its modification based on the algorithm Reversible Integer KLT [7].

VIII. CONCLUSIONS

A basic method for recursive color space transform of a group of correlated images is developed, based on the AC-KLT. It could be used as a basis for the development of:

- New algorithms for parallel processing of the images in the group, based on the RAC-KLT, which will enhance the calculation speed of the direct and inverse transforms;
- RAC-KLT algorithm with higher efficiency, based on the adaptive division of the processed group of images into groups of various length, where the correlation between the neighbor image couples is higher than a preset threshold. This approach will ensure higher reduction of the color components number for each group;
- New algorithms, aimed at various application areas.

Maximum efficiency for each algorithm could be achieved when the basic parameters of RAC-KLT are adapted depending on the application requirements in respect of accuracy, reversibility, execution time, implementation, methods for color parameters coding, etc.

REFERENCES

- [1] T. Reed (Ed.), *Digital Image Sequence Processing, Compression, and Analysis*, 2005, CRC Press.
- [2] R. Lucas, K. Plataniotis, *Color Image Processing: Methods and Applications*, 2007, Taylor & Francis.
- [3] M. Celebi, M. Lecca, B. Smolka (Eds.), *Color Image and Video Enhancement*, 2015, Springer.
- [4] M. Drew, S. Bergner, "Spatio-Chromatic Decorrelation for Color Image Compression", *Signal Processing: Image Communication*, Vol. 23, No. 8, Sept. 2008, pp. 599-609.
- [5] H. Abdi, L. Williams, "Principal Component Analysis", *Wiley Interdisciplinary Reviews: Computational Statistics*, Vol. 2, No. 4, 2010, pp. 433-459.
- [6] C. Maccone, "A simple introduction to the KLT (Karhunen-Loève Transform)", Chapter in *Deep Space Flight and Communications*, C. Maccone (Ed.), Springer, 2009, pp. 151-179.
- [7] P. Hao, Q. Shi, "Reversible integer KLT for progressive-to-lossless compression of multiple component images". In: *Intern. Conference on Image Processing (ICIP)*, Vol. 1, 2003, pp. 633-636.
- [8] Y. Chen, P. Hao, and A. Dang, "Optimal transform in perceptually uniform color space and its applications in image coding", In: *ICIAR 2004*, LNCS 3211, 2004, pp. 269-276.
- [9] A. Abadpour, S. Kasaei, Color PCA Eigenimages and their Application to Compression and Watermarking, *Image & Vision Computing*, Vol. 26, Issue 7, July 2008, pp. 878-890.
- [10] M. Minervini, C. Rusu, S. Tsafaris, "Unsupervised and Supervised Approaches to Color Space Transformation for Image Coding", *Proc. of the 21st IEEE Intern. Conference on Image Processing (ICIP'14)*, Paris, France, Oct. 27-30, 2014, pp. 5576-5580.
- [11] R. Starosolski, "New simple and efficient color space transformations for lossless image compression", *Journal of Visual Communication and Image Representation*, Vol. 25, No. 5, 2014, pp. 1056-1063.
- [12] M. Fairchild, *Color and Image Appearance Models*. John Wiley & Sons, 2005.
- [13] S. Singh, S. Kumar, "Novel Adaptive Color Space Transform and Application to Image Compression", *Signal Processing: Image Communication*, Vol. 26, No. 10, Nov. 2011, pp. 662-672.
- [14] P. Farrelle, Recursive. *Block Coding for Image Data Compression*, Springer, NY, 1990.
- [15] A. Suhre, K. Kose, A. Cetin, M. Gurcan, "Content-adaptive color transform for image compression", *Optical Engineering*, Vol. 50, No. 5, May 2011, pp. 057003-1 - 057003-7.
- [16] R. Kountchev, R. Kountcheva, "Image Color Space Transform with Enhanced KLT", Chapter in: *New Advances in Intelligent Decision Technologies*, K. Nakamatsu, G. Philips-Wren, L. Jain, R. Howlett (Eds.), Springer, 2009, pp. 171-182.
- [17] P. Ivanov, R. Kountchev, "Comparative analysis of Adaptive Color KLT and YCrCb for representation of color images", *Intern. Scientific Conf. on Information, Communication and Energy Systems and Technologies (ICEST'10)*, Ohrid, Macedonia, June 2010, SP I, pp. 29-32.
- [18] P. Ivanov, R. Kountchev, R. Mironov, "Algorithm for adaptive color KLT of images, based on histogram matching of the color components", *Intern. Scientific Conf. on Information, Communication and Energy Systems and Technologies (ICEST'11)*, Nis, Serbia, July 2011, Proc. of Papers, Vol. 1, SP I, pp. 5-8.
- [19] R. Kountchev, R. Kountcheva, "Color Space Transform for Correlated Images Based on the Recursive Adaptive KLT", *IARAS Intern. Journal of Signal Processing*, Vol. 2, 2017, pp. 72-80.